

Characterizations of the medium in jet quenching calculations.

A. Majumder^{1 a}

Department of Physics, Duke University, Durham, North Carolina 27708, USA.

Received: 14.09.08 / Revised version: date

Abstract. The modification of hard jets in dense matter has so far been described by four different formalisms based on perturbative QCD (pQCD). In these proceedings, we compare the various approximations made in these different schemes, especially those regarding the structure of the medium through which jets propagate. Following this, we highlight some of the major differences in the various physical processes contained in the different approaches.

PACS. 12.38.Mh, 11.10.Wx, 25.75.Dw

1 Introduction

One of the major discoveries of the heavy-ion program at the Relativistic Heavy-Ion Collider (RHIC) has been the observed suppression of high transverse momentum (high p_T) hadrons when compared to the yield of similar hadrons in p - p collisions (scaled up by the expected number of binary collisions) [1,2]. In p - p collisions, such hadrons are formed in the fragmentation of high p_T jets produced in hard scatterings. The presence of a dense medium influences the space-time development of the partonic shower from such jets and in turn leads to a medium modification of the final fragmentation to hadrons [3,4].

The presence of a hard jet introduces a large energy scale within the process and allows for a calculation of the modification using the methods of perturbative QCD (pQCD). Following the early attempts of Baier-Dokshitzer-Mueller-Peigne-Schiff and Zakharov (BDMPS-Z) [5,6,7,8,9,10,11], such calculations have grown in both sophistication and in the number of different observables that they are applied to. The majority of current approaches to the energy loss of light partons may be divided into four major schemes often referred to by the names of the original authors:

- Higher Twist scheme (HT) [12,13,14,15,16,17]
- Path integral approach to the opacity expansion by Armesto, Salgado and Wiedemann, (BDMPS-Z/ASW) [19,20,21,22,23,5,6,7,8,9,10]
- Finite temperature field theory approach by Arnold, Moore and Yaffe (AMY) [24,25,26,27,28]
- Reaction Operator approach to the opacity expansion by Gyulassy, Levai and Vitev, (GLV) [29,30,31,32,33]

^a *Present address:* Department of Physics, Ohio State University, Columbus, Ohio 43210, USA.

All these schemes utilize slightly different approximations regarding the various scales involved in the calculation and somewhat different quantitative pictures of the medium.

It will be demonstrated in the companion publication of Ref. [34], that, using these different formalisms to compute the medium modification of hard jets in an identical medium leads to rather similar predictions for experimental observables. In these proceedings, we outline the various differences between the theoretical formulations of the different schemes themselves. In Sect. 2, we present a brief introduction to the basic formalism and the definition of a medium modified fragmentation function. In Sect. 3, we present a brief review of how the different schemes compute the single gluon emission spectrum. In Sect. 4, we review how a single gluon emission spectrum is iterated in the different formalisms. We present concluding discussions in Sect. 5.

2 Hard scattering and the medium modified fragmentation function

In the collision of two heavy-ions, there occasionally occurs a hard scattering between two initial partons which leads to two back-to-back out-going partons with large transverse momentum. These encounter multiple scattering in the produced medium leading to a modification of the final distribution of hadrons emanating from these partons. In the computation of this modified distribution, all schemes utilize a factorized approach where the final cross section to produce a hadron h with transverse momentum p_T (rapidity between y and $y + dy$) may be expressed as a convolution of initial nuclear structure functions [$G_a^A(x_a), G_b^B(x_b)$, initial state nuclear effects such as shadowing and Cronin effect are understood to be included] to produce partons with momentum fractions x_a, x_b , a hard partonic cross section to produce a high transverse

momentum parton c with a transverse momentum \hat{p} and a medium modified fragmentation function for the final hadron $[\tilde{D}_c^h(z)]$,

$$\frac{d^2\sigma^h}{dyd^2p_T} = \frac{1}{\pi} \int dx_a dx_b G_a^A(x_a) G_b^B(x_b) \times \frac{d\sigma_{ab \rightarrow cX}}{dt} \frac{\tilde{D}_c^h(z)}{z}. \quad (1)$$

In the vicinity of mid-rapidity, $z = p_T/\hat{p}$ and $\hat{t} = (\hat{p} - x_a P)^2$ (P is the average incoming momentum of a nucleon in nucleus A). The entire effect of energy loss is concentrated in the calculation of the modification to the fragmentation function. The four models of energy loss are in a sense four schemes to estimate this quantity from perturbative QCD calculations.

While the terminology (medium modification) used to describe the change in the fragmentation function seems to indicate that the medium has influenced the actual process of the formation of the final hadrons from the partonic cloud, this is not the case. All computations simply describe the change in the gluon radiation spectrum from a hard parton due to the presence of the medium. The final hadronization of the hard parton is always assumed to occur in the vacuum after the parton, with degraded energy, has escaped from the medium. Note that some of the hard gluons radiated from the hard parton will also encounter similar “modification” in the medium and may endure vacuum hadronization after escaping from the medium. Differences between formalisms also arise in the inclusion of hadrons from the fragmentation of such sub-leading gluons: whereas in approaches which compute the change in the distribution of final partons (such as AMY) or the change in the distribution of final hadrons (such as HT), hadrons from sub-leading gluons are implicitly included, formalisms which compute the energy loss of the leading parton (such as ASW), do not include such sub-leading corrections.

To better appreciate the approximation schemes, one may introduce a set of scales (see Fig. 1): E or p^+ , the forward energy of the jet; Q^2 , the virtuality of the initial jet-parton; μ , the momentum scale of the medium and L , its spatial extent. Most of the differences between the various schemes may be reduced to the different relations between these various scales assumed by each scheme as well as by how each scheme treats or approximates the structure of the medium. In all schemes, the forward energy of the jet far exceeds the medium scale, $E \gg \mu$.

3 Single gluon emission and scattering in the medium

The first step in energy loss calculations is to compute the effect of a single gluon emission off a hard jet in the medium. The major theoretical differences between the various schemes arise in this calculation. It is in this step that differing assumptions regarding the medium (in different formalisms) are introduced. In the next section, the

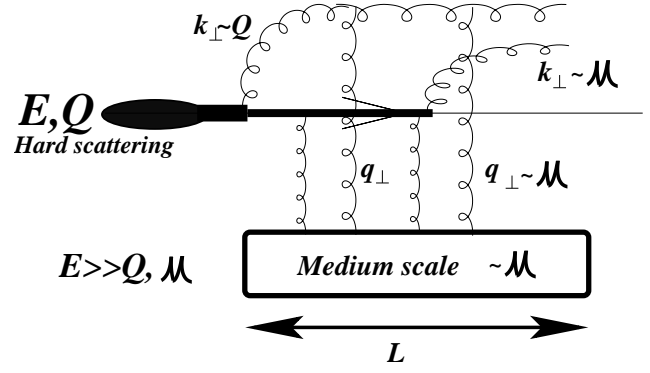


Fig. 1. A schematic picture of the various scales involved in the modification of jets in dense matter.

single emission kernel will be repeated to compute the effect of multiple emissions. In most cases, this involves a certain phenomenological picture and also introduces further differences between the different approaches.

3.1 Higher twist approach

The origin of the higher twist (HT) approximation scheme lies in the calculations of medium enhanced higher twist corrections to the total cross section in Deep-Inelastic Scattering (DIS) off large nuclei [35]. In those calculations, the authors computed a certain class of power corrections to the total leading twist cross sections, which, though suppressed by powers of the hard scale Q^2 , are enhanced by the extent of the medium. In the case of high p_T hadron production one identifies and resums corrections to the single hadron inclusive cross section.

One presupposes that the produced jet has a very large forward energy E which is much larger than its virtuality Q (which limits the transverse momentum of the radiated gluon, k_\perp), which in turn is much larger than the characteristic momentum scale in the medium μ , i.e., $E \gg k_\perp \gg \mu$. This hierarchy is then applied to the computation of multiple Feynman diagrams such as the one in Fig. 2. This diagram represents the process of a hard virtual quark produced in a hard collision, which then radiates a gluon and then scatters off a soft medium gluon with transverse momentum $q_\perp \sim \mu$ prior to exiting the medium and fragmenting into hadrons. Even at the order considered, there exist various other contributions which involve scattering of the initial quark, off the soft gluon field, prior to radiation as well as scattering of the radiated gluon itself. All such contributions are combined coherently to calculate the modification to the fragmentation function directly.

The hierarchy of scales allows one to use the collinear approximation to factorize the fragmentation function and its modification from the hard scattering cross section. Thus, even though such a modified fragmentation function is derived in DIS, it may be generalized to the kinematics of a heavy-ion collision. Diagrams where the outgoing parton scatters off the medium gluons, such as those in Fig. 2, produce a medium dependent additive contribution to the

vacuum fragmentation function, which may be expressed as,

$$\Delta D_i(z, Q^2) = \int_0^{Q^2} \frac{dk_{\perp}^2}{k_{\perp}^2} \frac{\alpha_s}{2\pi} \times \left[\int_{z_h}^1 \frac{dx}{x} \sum_{j=q,g} \left\{ \Delta P_{i \rightarrow j}(x, x_L, k_{\perp}^2) D_j^h \left(\frac{z_h}{x} \right) \right\} \right]. \quad (2)$$

In the above equation, $\Delta P_{i \rightarrow j}$ represents the medium modified splitting function of parton i into j where a momentum fraction x is left in parton j . The new momentum fraction $x_L = k_{\perp}^2 / (2P^- p^+ x(1-x))$ ¹, where the radiated gluon or quark carries away a transverse momentum k_{\perp} , P^- is the incoming momentum of a nucleon in the nucleus and p is the momentum of the virtual photon. The medium modified splitting functions may be expressed as a product of the vacuum splitting function $P_{i \rightarrow j}$ and a medium dependent factor,

$$\Delta \hat{P}_{i \rightarrow j} = P_{i \rightarrow j} \int_0^L d\zeta \frac{(N_c^2 - 1) \hat{q}}{2\pi C_R (k_{\perp}^2 + \langle q_{\perp}^2 \rangle)} f(\zeta, x_L). \quad (3)$$

Where, C_R is the representation dependent Casimir and N_c is the number of colours. The mean transverse momentum of the soft gluons is represented by the factor $\langle q_{\perp}^2 \rangle$. The distance ζ is the distance between the origin of the jet and the location of its scattering, which is limited by the length of the medium L . The function $f(\zeta, x_L)$ depends on the number of scatterings per radiated gluon included and encodes the in-medium interference effects such as the Landau-Pomeranchuk-Migdal effect [36, 37].

The factor \hat{q} encodes the soft gluon field in the medium, off which the jet encounters multiple scattering. It is given as [16]

$$\hat{q}(\zeta) = \frac{4\pi^2 \alpha_s C_R}{N_c^2 - 1} \int \frac{d\xi^+}{2\pi} \frac{d^2 \xi_{\perp} d^2 k_{\perp}}{(2\pi)^2} \times \exp \left[i \frac{q_{\perp}^2}{2p^+} \xi^+ - i \mathbf{p}_{\perp} \cdot \boldsymbol{\xi}_{\perp} \right] \times \langle F_{\sigma}^{\cdot}(\zeta + \xi^+/2, \boldsymbol{\xi}_{\perp}/2) F^{\sigma-}(\zeta - \xi^+/2, -\boldsymbol{\xi}_{\perp}/2) \rangle. \quad (4)$$

The transport coefficient is normalized by fitting to one data point and a model such as a Woods-Saxon distribution for cold matter or 3-D hydrodynamical evolution for hot nuclear matter is invoked for its variation with space-time location. The expectation $\langle \rangle$ is meant to be taken in the medium under consideration. Any space time dependence is essentially included in the implied expectation.

The gluons which contribute to \hat{q} do not have to be the entropy carriers of the system. In applications to cold nuclear matter, these gluons constitute the virtual gluon cloud inside the nucleons. In the case of a deconfined quark-gluon plasma, these may be the entropy carrying

¹ Throughout the HT portion of these proceedings, four-vectors will often be referred to using the light cone convention where $x^+ = x^0 + x^3$ and $x^- = (x^0 - x^3)/2$.

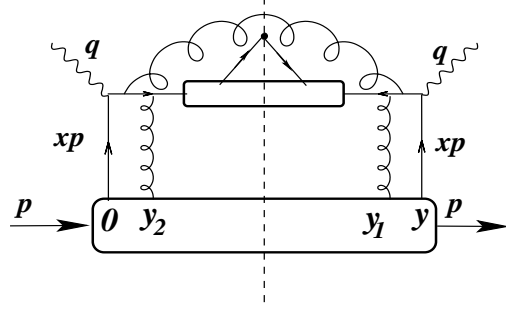


Fig. 2. A typical higher twist contribution to the modification of the fragmentation function in medium.

gluons or virtual excitations within these degrees of freedom. Which gluons the jet scatters off depends on the scale of the hard jet. It is immediately obvious from Eq. (4) that \hat{q} is a function of the jet energy p^+ . Note that p^+ is not integrated out. The actual dependence on p^+ depends on the medium in question. In the case of confined nuclear media, or a quark gluon plasma, the dependence is logarithmic. There is also a logarithmic dependence on the virtuality of the jet which sets in due to radiative corrections to the definition in Eq. (4). Also, as demonstrated in Ref. [18], \hat{q} may even possess a tensorial structure if the medium is not isotropic. In the calculations of the current manuscript, both the dependence on the energy and virtuality of the jet will be ignored. The medium will be assumed to be isotropic. The values of \hat{q} quoted should thus be considered as approximations to the full functional form.

3.2 Opacity expansion approach

Unlike the higher twist scheme, which is set up to directly calculate the final distribution of hadrons, opacity expansion approaches such as the Gyulassy-Levai-Vitev (GLV) scheme [29, 30, 31], and the Armesto-Salgado-Wiedemann (ASW) scheme [19, 20, 21, 22, 23] were constructed primarily to deal with the problem of energy loss of the leading parton in dense deconfined matter. Both these schemes assume that the medium is composed of heavy almost static color scattering centers which are well separated, in the sense that the mean free path of a jet $\lambda \gg 1/\mu$ the color screening length of the medium [4]. The opacity of the medium \bar{n} , which constitutes the expansion parameter of these calculations, quantifies the number of scattering centers seen by a jet as it passes through the medium, *i.e.*, $\bar{n} = L/\lambda$, where L is the thickness of the medium. The difference between the two approaches of the GLV and the ASW arise from how these tend to expand in n . In the GLV formalism, one constructs a recursive operator expansion in opacity, whereas in the ASW approach a path integral over opacity is formulated. The solution of the recursive operator approach in the GLV allows for an order-by-order expansion in opacity. The path-integral in the ASW approach has been solved analytically in two limits: the one-scattering approximation, equivalent to a first order in opacity calculation in the GLV approach and

in the multiple scattering approximation where all orders in opacity have been resummed. In this article (as well as in the companion [34] where results of calculation will be compared with experimental data), the focus will lie on the path integral approach of ASW.

The path integral approach for the energy loss of a hard jet propagating in a colored medium was first introduced in Ref. [8]. It was later demonstrated to be equivalent to the well known BDMPS approach [5,6,7] in the multiple scattering limit. ASW represents the current, most widespread, variant of this approach. In this scheme, a hard, almost on-shell parton traversing a dense medium full of heavy scattering centers will engender multiple transverse scatterings of order $\mu \ll p^+$. It will in the process split into an outgoing parton and a radiated gluon which will also scatter multiply in the medium. The radiated gluon, induced by the multiple scattering, has a transverse momentum $k_\perp \geq \mu$ (different from the HT approach). The propagation of the incoming (outgoing) partons as well as that of the radiated gluon in this background color field may be expressed in terms of effective Green's functions $[G(\mathbf{r}_\perp, z; \mathbf{r}'_\perp, z')]$ (for quark or gluon) which obey the obvious Dyson-Schwinger equation,

$$G(\mathbf{r}_\perp, z; \mathbf{r}'_\perp, z') = G_0(\mathbf{r}_\perp, z; \mathbf{r}'_\perp, z') - i \int_z^{z'} d\zeta \int d^2\mathbf{x} G_0(\mathbf{r}_\perp, z; \mathbf{x}, \zeta) A_0(\mathbf{x}, \zeta) G(\mathbf{x}, \zeta; \mathbf{r}'_\perp, z'), \quad (5)$$

where, G_0 is the free Green's function and A_0 represents the color potential of a scattering center in the medium. The solution for the above interacting Green's function involves a path ordered Wilson line which follows the potential from the location $[\mathbf{r}_\perp(z'), z']$ to $[\mathbf{r}_\perp(z), z]$. Expanding the expression for the radiation cross section to order A_0^{2n} corresponds to an expansion up to n^{th} order in opacity.

Taking the high energy limit and the soft radiation approximation ($x \ll 1$), one focuses on isolating the leading behavior in x that arises from the large number of interference diagrams at a given order of opacity. As a result of the approximations made, one recovers the BDMPS condition that the leading behavior in x is contained solely in gluon re-scattering diagrams. This results in the expression for the inclusive energy distribution for gluon radiation off an in-medium produced parton as [20],

$$x \frac{dI}{dx} = \frac{\alpha_s C_R}{(2\pi)^2 x^2} 2\text{Re} \int_{\zeta_0}^{\infty} dy_i \int_{y_i}^{\infty} d\bar{y}_i \int_0^{\chi x p^+} d\mathbf{u} \int d\mathbf{k} e^{-i\mathbf{k} \cdot \mathbf{u} - \frac{1}{2} \int d\zeta n(\zeta) \sigma(\mathbf{u})} \times \frac{\partial^2}{\partial y \partial u} \int_{\mathbf{y}=0=\mathbf{r}(y_i)}^{\mathbf{u}=\mathbf{r}(\bar{y})} \mathcal{D}r e^{i \int d\zeta \frac{x p^+}{2} \left(|\dot{\mathbf{r}}|^2 - \frac{n(\zeta) \sigma(\mathbf{r})}{ix p^+} \right)}, \quad (6)$$

where, as always, k_\perp is the transverse momentum of the radiated gluon and $x p^+$ is its forward momentum. The vectors \mathbf{y} and \mathbf{u} represent the transverse locations of the emission of the gluon in the amplitude and the complex

conjugate whereas y_i and \bar{y}_i represent the longitudinal positions. The density of scatterers in the medium at location ζ is $n(\zeta)$ and the scattering cross section is $\sigma(r)$. In this form, the opacity is obtained as $\int n(\zeta) d\zeta$ over the extent of the medium.

Numerical implementations of this scheme have focused on two separate regimes. In one case, $\sigma(r)$ is replaced with a dipole form $C r^2$ and one solves the harmonic oscillator like path integral. This corresponds to the case of multiple soft scatterings of the hard probe. In the limit of a static medium with a very large length, one obtains the simple form for the radiation distribution [38],

$$\omega \frac{dI}{d\omega} \simeq \frac{2\alpha_s C_R}{\pi} \begin{cases} \sqrt{\frac{\omega_c}{2\omega}} & \text{for } \omega < \omega_c, \\ \frac{1}{12} \left(\frac{\omega}{\omega_c} \right)^2 & \text{for } \omega > \omega_c. \end{cases} \quad (7)$$

Where $\omega_c = \int d\zeta \zeta \hat{q}(\zeta)$ is called the characteristic frequency of the radiation. Up to constant factors, this is equal to mean energy lost in the medium ($\langle E \rangle$) *i.e.*, $\omega_c \simeq 2\langle E \rangle / (\alpha_s C_R)$. For a static medium, the integral defining ω_c may be performed to obtain $\omega_c = \hat{q} L^2 / 2$, where L is the length of the medium and \hat{q} is the jet transport coefficient, defined as the transverse momentum picked up by a hard jet per unit length. In actual numerical implementations, the mean \hat{q} (or the \hat{q} at a well defined location and time) is the only tunable parameter when comparing with experimental data. For a dynamical medium of finite extent, the characteristic frequency and the overall mean transverse momentum gained by the jet ($\hat{q}L$) will have to be estimated based on an Ansatz for the space time distribution of the transport parameter \hat{q} (see Ref. [34] for further details).

In the other extreme, one expands the exponent as a series in $n\sigma$; keeping only the leading order term corresponds to the picture of gluon radiation associated with a single scattering. In this second form, the analytical results of the ASW scheme formally approach those of the GLV reaction operator expansion [38]. In either case, the gluon emission intensity distribution has been found to be rather similar, once scaled with the characteristic frequency in each case.

3.3 Finite temperature field theory approach

In this scheme, often referred to as the Arnold-Moore-Yaffe (AMY) approach, the energy loss of hard jets is considered in an extended medium in equilibrium at asymptotically high temperature $T \rightarrow \infty$. Due to asymptotic freedom, the coupling constant $g \rightarrow 0$ at such high temperatures and a power counting scheme emerges from the ability to identify a hierarchy of parametrically separated scales $T \gg gT \gg g^2 T$ *etc.* In this limit, it becomes possible to construct an effective field theory of soft modes, *i.e.*, $p \sim gT$ by summing contributions from hard loops with $p \sim T$, into effective propagators and vertices [39].

One assumes a hard on-shell parton, with energy several times that of the temperature, traversing such a medium,

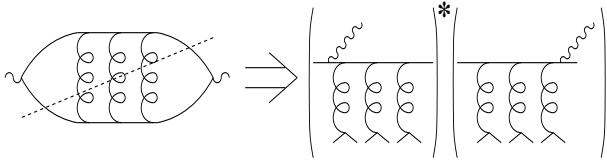


Fig. 3. A typical cut diagram in the AMY formalism.

undergoing soft scatterings with momentum transfers $\sim gT$ off other hard partons in the medium. Such soft scatterings induce collinear radiation from the parton, with a transverse momentum of the order of gT . The formation time for such collinear radiation $\sim 1/(g^2T)$ is of the same order of magnitude as the mean free time between soft scatterings [25]. As a result, multiple scatterings of the incoming (outgoing) parton and the radiated gluon need to be considered to get the leading order gluon radiation rate. One essentially calculates the imaginary parts of infinite order ladder diagrams such as those shown in Fig. 3; this is done by means of integral equations [26].

The imaginary parts of such ladder diagrams yield the $1 \rightarrow 2$ decay rates of a hard parton (a) into a radiated gluon and another parton (b) Γ_{bg}^a . These decay rates are then used to evolve hard quark and gluon distributions from the initial hard collisions, when they are formed, to the time when they exit the medium, by means of a Fokker-Planck like equation [27], which is written schematically as,

$$\frac{dP_a(p)}{dt} = \int dk \sum_{b,c} \left[P_b(p+k) \frac{d\Gamma_{ac}^b(p+k,p)}{dkdt} - P_a(p) \frac{d\Gamma_{bc}^a(p,k)}{dkdt} \right]. \quad (8)$$

The use of an effective theory for the description of the medium and the propagation of the jet, makes this approach considerably more systematic than the two previous approaches: both the properties of the jet and the medium are described using the same hierarchy of scales. It remains the only approach to date which naturally includes partonic feedback from the medium, *i.e.*, processes where a thermal quark or gluon may be absorbed by the hard jet ². In contrast to ASW and HT, this approach also (naturally) includes flavor changing interactions in the medium. Elastic energy loss may also be incorporated within the same basic formalism [41]. However, since the AMY scheme assumes a thermalized partonic medium, its applicability is somewhat limited: It cannot compute the quenching of jets in the confined sector. As a result, energy loss in cold confined nuclear matter as well as in

² While an attempt to include such effects in the higher twist formalism have been made in Ref. [40], these remain as phenomenological extensions and have not been included in this manuscript.

the hadronic phase of heavy-ion collisions cannot be computed in this model. The off-shellness or virtuality of all jets is considered to be similar to that of hard partons in the medium, as a result, interference between vacuum and medium induced radiations is also not considered.

In realistic calculations, the temperature of the medium is usually set by the underlying hydrodynamic simulation (see Ref. [34] for details). While in the HT or ASW formalisms, an Ansatz is made for the one tunable parameter \hat{q} and its relation to T , in the AMY formalism, \hat{q} may be calculated directly from a knowledge of the temperature and the strong coupling constant g (or α_s). This is due to the precise picture of the medium used: that of a hot plasma of quarks and gluons. In realistic simulations, the coupling is, in principle, unknown and becomes the primary fit parameter. This is then fit by comparison to one data point.

4 Multiple gluon emissions

In the preceding section, the effect of a single gluon emission, stimulated by scattering in the medium, was considered. In order to compute the final spectrum of hadrons, this single emission kernel has to be repeated to account for multiple gluon emissions and folded with a non-perturbative fragmentation function. Even in this procedure, the different schemes employ different methods: The HT scheme starts with a fragmentation function at a lower scale μ and evolves this distribution up to a higher scale. The ASW scheme, considers a finite energy lost by the leading parton in multiple unrelated events by means of a Poisson distribution and folds the outgoing parton with a vacuum fragmentation function with a shifted momentum fraction z . The AMY formalism considers the evolution of an initial distribution of hard partons with time in the medium using the Fokker-Planck equation afforded by Eq. 8 and final also uses a vacuum fragmentation function with a shifted momentum fraction z .

4.1 Higher twist scheme

In subsection 3.1, the medium modified fragmentation function calculated in Eq. (3) included only one gluon emission in the medium. Any remaining gluon emissions occurred in the vacuum and were included in the renormalization of the vacuum fragmentation function. Unlike the remaining formalisms, the results from just the single gluon emission in the medium yield a medium modified fragmentation function and are already comparable with experiment.

In reality, one expects multiple emissions to occur in the medium, followed by escape into the vacuum and further emissions in the vacuum. One starts with a vacuum fragmentation function at a low scale μ_{low} and insists that the parton exits the medium with a certain virtuality μ . Emissions from the scale μ_{low} up to the scale μ may be included by using the standard vacuum Dokshitzer-Gribov-Lipatov-Altarelli-Parisi (DGLAP) evolution equations [42, 43, 44].

Emissions in the medium account for the remaining evolution from the scale μ up to the scale Q . To compute this in-medium evolution, the medium modified fragmentation function from single gluon emission in Eq. (3) is now generalized to an evolution equation in virtuality of the propagating parton (see Ref. [45] for details), i.e.,

$$\frac{\partial D_q^h(z, M^2; p^+)|_{\zeta_i}^{\zeta_f}}{\partial \log(M^2)} = \int_z^1 dy \int_{\zeta_i}^{\zeta_f} d\zeta P_{i \rightarrow j} \frac{(N_c^2 - 1)\hat{q}(\zeta)}{2\pi C_R(k_\perp^2 + \langle q_\perp^2 \rangle)} \times f(\zeta, x_L, y) D_q^h\left(\frac{z}{y}, M^2, q^- y\right) \Big|_{\zeta}^{\zeta_f}. \quad (9)$$

The initial conditions to this differential equation are provided by the fragmentation functions at the scale μ . The final resulting medium modified fragmentation functions includes both vacuum and in-medium induced emissions from the scale Q down to the scale μ . Further emissions occur solely in the vacuum. This medium modified fragmentation function may now be convoluted with the cross section to produce a hard parton [as in Eq. (1)] to find the final distribution of hadrons. Computation of the medium modified fragmentation function in an evolving medium such as the deconfined matter formed in a quark-gluon plasma involves further calculational details presented in Ref. [34]. As the HT formalism is setup to directly calculate the final modified fragmentation function, it offers the simplest and most direct extension to the study of multi-hadron observables [46].

4.2 Opacity expansion scheme

In subsection 3.2, the opacity expansion was used to calculate the differential spectrum for single gluon radiation from a hard parton. The calculations were carried out in the soft gluon limit *i.e.*, $\omega \rightarrow 0$. The next step is to calculate the probability for the leading hard parton to radiate off a finite energy $\Delta E = \epsilon P^+$. After losing this energy, the degraded hard parton escapes the medium and fragments in vacuum into a shower of hadrons.

For the parton to lose a finite fraction of its forward energy, multiple gluon emissions are required. Each such emission at a given opacity is assumed to be independent and a probabilistic scheme is set up, wherein, the jet loses an energy fraction ΔE in n tries with a Poisson distribution [22, 47],

$$P_n(\epsilon, P^+) = \frac{e^{-\langle N_g \rangle}}{n!} \Pi_{i=1}^n \left[\int dx_i \frac{dN_g}{dx_i} \right] \delta(\epsilon - \sum_{i=1}^n x_i), \quad (10)$$

where, $\langle N_g \rangle$ is the mean number of gluons radiated per coherent interaction set. Summing over n gives the probability $P(\epsilon)$ for an incident jet to lose a momentum fraction ϵ due to its passage through the medium.

This probability distribution is then used to model a medium modified fragmentation function, by shifting the

energy fraction available to produce a hadron as well as accounting for the phase space available after energy loss (The fragmentation function used is a vacuum fragmentation function). The medium modified fragmentation function is thus defined as [22, 47],

$$\tilde{D}(z, Q^2) = \int_0^1 d\epsilon P(\epsilon) \frac{D\left(\frac{z}{1-\epsilon}, Q^2\right)}{1-\epsilon}. \quad (11)$$

The above, modified fragmentation function is then used in a factorized formalism as in Eq. (1) to calculate the final hadronic spectrum. Additional details related to the computation of the energy loss probability distribution are given in Ref. [34].

4.3 Finite temperature field theory scheme

In subsection 3.3, the computation of the rates of parton splitting and merging in a thermalized deconfined medium were calculated. Based on these rates, a Fokker-Plank equation was motivated which computed the change in the distribution of hard partons with time spent propagating through a medium. If the initial distribution is taken from the cross-section to produce a hard parton as in Eq. (1) and the time spent in the medium is estimated based on the production point and the direction of propagation, this equation will yield the distribution of hard partons as they exit the deconfined medium. In the AMY scheme, these partons are no longer expected to interact with the hadronic plasma and thus do not lose energy in the hadronic phase.

The final hadron spectrum at high p_T is obtained by the fragmentation of jets in the vacuum after their passing through the medium. In this approach, one calculates the medium modified fragmentation function by convoluting the vacuum fragmentation functions with the hard parton distributions, at exit, to produce the final hadronic spectrum [28],

$$\tilde{D}_j^h(z, \mathbf{r}_\perp, \phi) = \sum_{j'} \int dp_{j'} \frac{z'}{z} D_{j'}^h(z') P(p_{j'} | p_j, \mathbf{r}_\perp, \phi). \quad (12)$$

In the equation above, the sum over j' is the sum over all parton species. The two momentum fractions are $z = p_h/p_j$ and $z' = p_h/p_{j'}$, where p_j and $p_{j'}$ are the momenta of the hard partons immediately after the hard scattering and prior to exit from the medium and p_h is the final hadron momentum. The quantity $P(p_{j'} | p_j, \mathbf{r}_\perp, \phi)$ represents the solution to Eq. (8), which is the probability of obtaining a given parton j' with momentum $p_{j'}$ when the initial condition is a parton j with momentum p_j . The above integral depends implicitly on the path taken by the parton and the medium profile along that path, which in turn depends on the location of the origin \mathbf{r}_\perp of the jet and its propagation angle ϕ with respect to the reaction plane. Therefore, one must convolve the above expression over all transverse positions \mathbf{r}_\perp and directions ϕ . Details of this procedure are presented in the companion paper of Ref. [34].

5 Discussions and conclusions

In these proceedings, the different underlying theoretical mechanisms used in some of the prevalent jet energy loss calculations have been outlined. Specific attention was paid to how each jet resolves the medium and on the property of the medium which controls the modification of the hard jet. In all cases, the jet modification formalisms may be reduced to a form which depends on only one parameter: this is the transport coefficient \hat{q} defined as the transverse momentum gained by a hard parton per unit length traversed in a dense medium. While in the ASW formalism, \hat{q} is the sole tunable parameter, in the HT formalism, \hat{q} depends on the gluon field strength correlation [Eq. 4] and may be calculated from a knowledge of the temperature and the coupling constant α_s in the AMY formalism.

In all cases, the jet is assumed to fragment outside the medium. As a result, all formalisms use a medium modified fragmentation function, which uses a vacuum fragmentation function as input. While in the ASW and the HT formalisms, the modification is computed in both deconfined and confined phases, due to the assumptions made in the AMY formalism, the modification in this formalism occurs only in the deconfined phase. The modification in the confined phase is assumed to be small and ignored. While both the HT and the ASW formalisms include contributions from interference with vacuum radiation, these are ignored in the AMY scheme. The AMY approach however includes contributions from thermal feedback which has so far not been straightforwardly included in the HT and ASW formalisms. The consistent setup of the AMY formalism also allows for the most natural extension to include elastic energy loss [41]. While in the strict interpretation of heavy scattering centers in the ASW (and GLV) formalism, elastic energy loss is identically zero, the inclusion of elastic loss requires additional assumptions about the medium in the HT approach. Extensions to the GLV formalism to include mobile scattering centers, and thus, both include elastic energy loss [33] and modify the formulation of radiative energy loss [48] are currently underway. Similar extensions in the HT approach are also being carried out [49]. However, given the incomplete setup in different formalisms, elastic energy loss was not discussed in these proceedings, nor will be included in the realistic comparisons presented in Ref. [34].

While the description of the different formalisms in these proceedings have not included the effect of a dynamical medium, realistic calculations of jet modification in heavy-ion collisions do include such effects. The modification depends on the path traversed by a given jet. This in turn depends on the origin of the jet and the direction of travel in the medium. The details related to this problem, as it applies to the different formalisms will be presented in the companion paper [34]. As a result, comparisons to experimental data will also be carried out in this reference as well.

6 Acknowledgments

This work was supported in part by the U. S. Department of Energy, under grant numbers DE-FG02-05ER41367 and DE-FG02-01ER41190. The author thanks S. A. Bass, C. Gale, B. Müller, C. Nonaka, G.-Y. Qin, T. Renk and J. Ruppert for discussions. The author thanks U. Heinz for a careful reading of the manuscript and for discussions.

References

1. K. Adcox *et al.* [PHENIX Collaboration], Phys. Rev. Lett. **88**, (2002) 02230.
2. C. Adler *et al.* [STAR Collaboration], Phys. Rev. Lett. **89** (2002) 202301.
3. X. N. Wang and M. Gyulassy, Phys. Rev. Lett. **68** (1992) 1480.
4. M. Gyulassy and X. N. Wang, Nucl. Phys. B **420** (1994) 583.
5. R. Baier, Y. L. Dokshitzer, A. H. Mueller, S. Peigne and D. Schiff, Nucl. Phys. B **483** (1997) 291;
6. R. Baier, Y. L. Dokshitzer, A. H. Mueller and D. Schiff, Phys. Rev. C **58** (1998) 1706.
7. R. Baier, Y. L. Dokshitzer, A. H. Mueller, S. Peigne and D. Schiff, Nucl. Phys. B **484** (1997) 265 [arXiv:hep-ph/9608322].
8. B. G. Zakharov, JETP Lett. **63** (1996) 952 [arXiv:hep-ph/9607440].
9. B. G. Zakharov, JETP Lett. **65** (1997) 615 [arXiv:hep-ph/9704255].
10. B. G. Zakharov, Phys. Atom. Nucl. **61** (1998) 838 [Yad. Fiz. **61** (1998) 924] [arXiv:hep-ph/9807540].
11. R. Baier, D. Schiff and B. G. Zakharov, Ann. Rev. Nucl. Part. Sci. **50** (2000) 37.
12. X. f. Guo and X. N. Wang, Phys. Rev. Lett. **85** (2000) 3591;
13. X. N. Wang and X. f. Guo, Nucl. Phys. A **696** (2001) 788.
14. B. W. Zhang and X. N. Wang, Nucl. Phys. A **720** (2003) 429 [arXiv:hep-ph/0301195].
15. A. Majumder, E. Wang and X. N. Wang, Phys. Rev. Lett. **99** (2007) 152301 [arXiv:nucl-th/0412061].
16. A. Majumder and B. Muller, Phys. Rev. C **77** (2008) 054903 [arXiv:0705.1147 [nucl-th]].
17. A. Majumder, R. J. Fries and B. Muller, Phys. Rev. C **77** (2008) 065209 [arXiv:0711.2475 [nucl-th]].
18. A. Majumder, B. Muller and S. A. Bass, Phys. Rev. Lett. **99** (2007) 042301 [arXiv:hep-ph/0611135].
19. U. A. Wiedemann, Nucl. Phys. B **582** (2000) 409 [arXiv:hep-ph/0003021].
20. U. A. Wiedemann, Nucl. Phys. B **588** (2000) 303 [arXiv:hep-ph/0005129].
21. C. A. Salgado and U. A. Wiedemann, Phys. Rev. Lett. **89** (2002) 092303 [arXiv:hep-ph/0204221].
22. C. A. Salgado and U. A. Wiedemann, Phys. Rev. D **68** (2003) 014008 [arXiv:hep-ph/0302184].
23. N. Armesto, C. A. Salgado and U. A. Wiedemann, Phys. Rev. Lett. **94** (2005) 022002 [arXiv:hep-ph/0407018].
24. P. Arnold, G. D. Moore and L. G. Yaffe, JHEP **0011** (2000) 001 [arXiv:hep-ph/0010177].
25. P. Arnold, G. D. Moore and L. G. Yaffe, JHEP **0111** (2001) 057 [arXiv:hep-ph/0109064].

26. P. Arnold, G. D. Moore and L. G. Yaffe, JHEP **0206**, 030 (2002) [arXiv:hep-ph/0204343].
27. S. Jeon and G. D. Moore, Phys. Rev. C **71** (2005) 034901 [arXiv:hep-ph/0309332].
28. S. Turbide, C. Gale, S. Jeon and G. D. Moore, Phys. Rev. C **72** (2005) 014906 [arXiv:hep-ph/0502248].
29. M. Gyulassy, P. Levai and I. Vitev, Nucl. Phys. B **571**, 197 (2000) [arXiv:hep-ph/9907461].
30. M. Gyulassy, P. Levai and I. Vitev, Nucl. Phys. B **594** (2001) 371 [arXiv:nucl-th/0006010].
31. M. Gyulassy, P. Levai and I. Vitev, Phys. Lett. B **538** (2002) 282 [arXiv:nucl-th/0112071].
32. M. Djordjevic and M. Gyulassy, Nucl. Phys. A **733** (2004) 265 [arXiv:nucl-th/0310076].
33. S. Wicks, W. Horowitz, M. Djordjevic and M. Gyulassy, Nucl. Phys. A **784** (2007) 426 [arXiv:nucl-th/0512076].
34. S. A. Bass, *et. al.*, *these proceedings*.
35. J. w. Qiu and G. Sterman, Nucl. Phys. B **353** (1991) 137; Nucl. Phys. B **353** (1991) 105.
36. L. D. Landau and I. Pomeranchuk, Dokl. Akad. Nauk Ser. Fiz. **92** (1953) 535.
37. A. B. Migdal, Phys. Rev. **103** (1956) 1811.
38. U. A. Wiedemann, Nucl. Phys. A **690**, 731 (2001) [arXiv:hep-ph/0008241].
39. E. Braaten and R. D. Pisarski, Phys. Rev. Lett. **64** (1990) 1338.
40. E. Wang and X. N. Wang, Phys. Rev. Lett. **87**, 142301 (2001) [arXiv:nucl-th/0106043].
41. G. Y. Qin, J. Ruppert, C. Gale, S. Jeon, G. D. Moore and M. G. Mustafa, Phys. Rev. Lett. **100** (2008) 072301 [arXiv:0710.0605 [hep-ph]].
42. V. N. Gribov and L. N. Lipatov, Sov. J. Nucl. Phys. **15** (1972) 438 [Yad. Fiz. **15** (1972) 781].
43. Y. L. Dokshitzer, Sov. Phys. JETP **46** (1977) 641 [Zh. Eksp. Teor. Fiz. **73** (1977) 1216].
44. G. Altarelli and G. Parisi, Nucl. Phys. B **126** (1977) 298.
45. A. Majumder, *to appear*.
46. A. Majumder and X. N. Wang, Phys. Rev. D **70**, 014007 (2004) [arXiv:hep-ph/0402245].
47. K. J. Eskola, H. Honkanen, C. A. Salgado and U. A. Wiedemann, Nucl. Phys. A **747**, 511 (2005) [arXiv:hep-ph/0406319].
48. M. Djordjevic and U. Heinz, Phys. Rev. C **77** (2008) 024905 [arXiv:0705.3439 [nucl-th]]; Phys. Rev. Lett. **101** (2008) 022302 [arXiv:0802.1230 [nucl-th]].
49. X. N. Wang, Phys. Lett. B **650** (2007) 213 [arXiv:nucl-th/0604040]; A. Majumder, *to appear*.